

Article

Sustainable Adaptive Cycle Pavements Using Composite Foam Concrete at High Altitudes in Central Europe

Martin Decky ¹, Katarina Hodasova ^{1,*}, Zuzana Papanova ²  and Eva Remisova ¹ 

¹ Department of Highway and Environmental Engineering, University of Zilina, Univerzitna 8215/1, 010 26 Zilina, Slovakia; martin.decky@uniza.sk (M.D.); eva.remisova@uniza.sk (E.R.)

² Department of Structural Mechanics and Applied Mathematics, University of Zilina, Univerzitna 8215/1, 010 26 Zilina, Slovakia; zuzana.papanova@uniza.sk

* Correspondence: katarina.hodasova@uniza.sk; Tel.: +421-9480-66540

Abstract: Climate pavement adaptability is an integral part of a holistic concept of road design, construction, and pavement management. One of the possibilities for fulfilling the mentioned author's premise in sustainable cycle pavements in the cold region of Central Europe is using composite foam concrete (CFC). To establish the credibility of the design of these pavements, we objectified the correlation dependencies of average annual air temperatures and frost indexes, for altitude regions from 314 to 858 m in the period 1971 to 2020, at its height above sea level. As part of the research on the increase in tensile strength during bending of CFC, extensive laboratory measurements were carried out and validated by isomorphic models of real roads, which enabled an increase in tensile strength during bending from 0.376 to 1.370 N·mm⁻² for basalt reinforcing mesh. The research results, verified through FEM (Finite Element Method) models of cycle pavements, demonstrated a possible reduction of total pavement thickness from 56 to 38 cm for rigid pavements and 48 to 38 cm for flexible pavements.

Keywords: foam concrete; reinforcing basalt mesh; annual air temperature; modulus of elasticity; cycle pavement



Citation: Decky, M.; Hodasova, K.; Papanova, Z.; Remisova, E. Sustainable Adaptive Cycle Pavements Using Composite Foam Concrete at High Altitudes in Central Europe. *Sustainability* **2022**, *14*, 9034. <https://doi.org/10.3390/su14159034>

Academic Editor: Jozef Švajlenka

Received: 10 June 2022

Accepted: 20 July 2022

Published: 23 July 2022

Publisher's Note: MDPI stays neutral with regard to jurisdictional claims in published maps and institutional affiliations.



Copyright: © 2022 by the authors. Licensee MDPI, Basel, Switzerland. This article is an open access article distributed under the terms and conditions of the Creative Commons Attribution (CC BY) license (<https://creativecommons.org/licenses/by/4.0/>).

1. Introduction

Higher Education Institutions have the mandate of promoting sustainability by addressing the United Nation's 2030 Agenda [1]. The Sustainable Development Goals (SDGs) are a universal set of seventeen goals and targets, with accompanying indicators, which were agreed upon by UN member states to frame their policy agendas for the fifteen-year period from 2015 to 2030 [2]. All of the objectives of Agenda 2030, emphasizing science, technology, and innovation (STI) are most welcome, but achieving desired outcomes by 2030 will require a deep understanding of how to maximize the contributions of STI [3]. Global developments in construction give sustainability a crucial role in the overall healthy functioning of society as well as the whole environment. Modern Methods of Construction (MMC) represent a response to the sustainability trend since they bring faster construction and better environmental, energy, and economic parameters [4]. Kibert [5] laid down the foundation for Sustainable Construction (SC) practice, and established SC around resource minimization and reuse, use of renewable and recyclable resources, and minimizing carbon footprint. Vanegas and Pearce [6] presented SC based on resource depletion and degradation, impact on the built environment and human health, Braungart and McDonough [7] offered the cradle-to-cradle definition, and Pulaski [8] presented a comprehensive approach towards sustainability in construction operation, Mallick and El-Korchi [9].

In the context of road adaptive design [10,11], including pavements for walking and cycling journeys, forming 20–40% of the total journeys in the European Union [12,13], it is possible to take these data into account at an early stage [14]. Other examples of the diversity of innovative solutions point to their possible use and improvement on the impact

on the living environment and sustainability already present in the pavement design and management phase [15,16]. The authors have long devoted themselves to a holistic concept of design, construction, and pavement management, of which climate adaptability is also an integral part [17,18] along with saving non-renewable resources [19,20]. One of the first approaches applied was decreasing the energy consumption during production by using new energy-efficient technologies, using reclaimed materials [21,22], incorporating new types of materials [23], waste recovery [24] as well as by modifying the technology e.g., by decreasing the processing temperature (using additives or foaming technologies [25,26]). Their use has successfully shown a positive impact on non-renewable cumulative energy demand and global warming potential. However, an important requirement for the use remains to ensure the quality, durability, and service longevity of the produced transport infrastructure.

For the last 10 years, authors in the field of STI pavement materials have been mainly researching and improving the properties of foam concrete [11,21,22,27] for the purposes of its application in pavement construction. Lightweight foamed concrete (LWFC) has found its first application in building constructions as roof slopes and floor leveling, later in lightweight blocks, thermal and acoustic insulation, void filling and trench reinstatement, slope stabilization, road subbase, encapsulate bridge piers, backfilling the voids behind the tunnel lining, sports fields, soft ground engineered arresting system for airports [28,29]. LWFC from the point of pavement application has advantageous properties including low self-weight [30], which is important in refurbishment operations; it also works to lessen the loads, establish thermal insulating characteristics [31,32], promote fire resistance [33], and reduces the cost of production and thus cost during the construction and workability [33,34]. Foam concrete has a low weight (250 to 900 kg·m⁻³), minimal aggregate consumption (significant saving in natural resources), controlled low strength (0.3 to 5 MPa), and excellent thermal and acoustic insulation properties (thermal conductivity of 0.058 to 0.26 W/m·K). Its specific characteristic is that it contains closed air pores that reduce its volumetric weight. FC allows also for the incorporation of recycled and secondary materials (demolition fines or conditioned fly ash).

Recently, LWFC has also begun to find applications in civil engineering structures in Central Europe, especially at higher altitudes requiring increased protection against the adverse effects of frost [35–38]. In the present article, the authors present the latest results of their research in the field by increasing the tensile strength in bending LWFC through the application of various reinforcement nets. Optimized design of the composite foam concrete pavement layer (use of basalt reinforcement mesh) in conjunction with credible data on climatic characteristics and validated FEM models enable their application in accordance with the requirements of the Slovak Road Act [39]. Until the middle of the 20th century, methods based on limited deflection [40,41] and limited shear failure prevailed in the assessment of roads [42]. However, these assumptions are not accurate, in pavement materials, stress leads to elastic, viscous, plastic, and viscoelastic deformations; therefore, the materials behave nonlinearly [43]. The finite element method (FEM) for the analysis of flexible pavements was first applied by Duncan [44], which allowed the assessment of pavements considering the nonlinear properties of pavement materials and therefore, the use of FEM is becoming popular in determining their stresses and deflections [45–47]. This article presents, for the first time in Central Europe, a FEM model of a cycle pavement using a base layer of composite foam concrete, the relevant mechanical characteristics of which were found during the 10 years of research carried out at the authors' workplace [48–50].

The paper presents the results of the research enabling sustainable, adaptive cycle pavements design (SACD) using composite foam concrete at high altitudes in Central Europe (CE). The territorial definition of the term CE may seem straightforward at first sight, but in reality, it is not. The authors, therefore, present in a separate chapter the development and the currently established perception of CE [51–54] as well as their definition of the territory of CE. The paper also provides an overview of the highest and lowest permanent settlements of CE individual countries, whereas, for the purposes of the SACD, the authors divided the altitudes of inhabited settlements in Central Europe into four categories, namely

0–300, 301–670, 671–1000, and above 1000 m above sea level. The paper considers only altitudes above 330 m, with emphasis on settlements above 670 m, while a case study for the highest permanently inhabited village in Slovakia, Demanovska Dolina with an altitude of 1109 m above sea level, is given.

2. Methods

In this article, priority attention is focused on the following research activities carried out by the authors:

- Statistical analyses of the evolution of relevant climatic characteristics of Central Europe between 1971 and 2020 for altitudes above 330 m a.s.l.;
- Determination of flexural strength of isomorphic models with foam concrete according to STN EN 12390-5:2020 Testing hardened concrete. Part 5: Flexural strength of test specimens [55];
- Verification of the accuracy of laboratory tests on homomorphic models of real pavement structure [41,42];
- FEM models are used to validate the modeling methodology and to create a FEM model of the pavements of interest;
- Analytical models in Central European conditions binding for design of asphalt and cement concrete (CC) pavements with reinforces FC 500 base course.

2.1. Territorial Definition of the Central European Area and the Range of Heights

The development of the territorial delimitation of Central Europe from 1917 to 2022 is shown in Figure 1. It presents the current delimitation of the SE [54] with redrawn boundaries from [51]. Many geographical names either lack or lose their precise meaning, and the term Central Europe is a typical example. The development of the perception of Central Europe according to different authors is also shown in Figure 1.

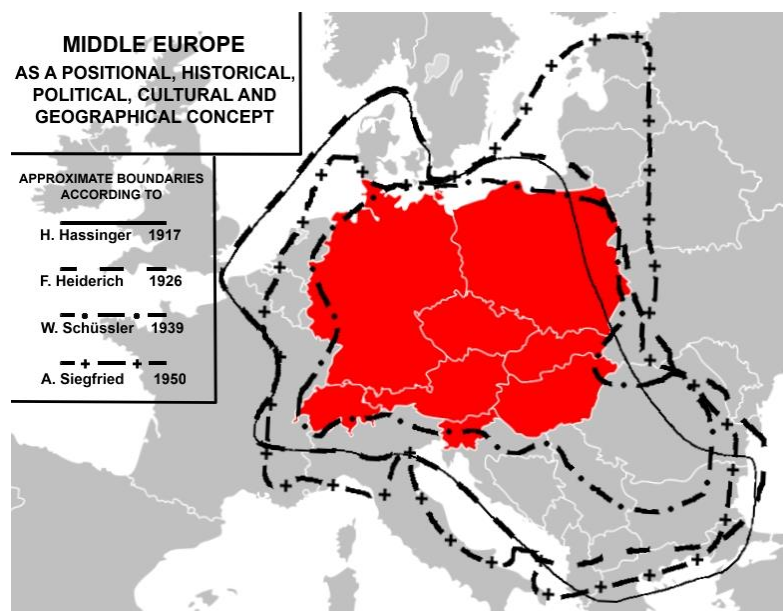


Figure 1. Development of the territorial delimitation of Central Europe from 1917 to 2022, redrawn boundaries from [51] to the current delimitation of the SE [54].

The location of the geographical center of Europe depends on the delimitation of Europe's borders. Particularly on whether remote islands are included to define the extreme points of Europe and on the method of calculating the result. Therefore, several places claim to host this hypothetical center: the town of Kremnicke Bane or the neighboring town Krahule, near Kremnica, in central Slovakia; the town of Rakhiv, or the town of Dilove, near Rakhiv, in western Ukraine; the town of Girija, near Vilnius, in Lithuania; a point on

the island of Saaremaa, in Estonia; a point near Polotsk, or in Vitebsk, or near Babruysk, or Lake Sho, in Belarus; a point near the town of Tallya, in northeastern Hungary (Figure 2a). The towns of Krahule and Kremnicke Bane are generally understood by Slovak authors as the geometric center of continental Europe, as well as by foreign authors [52,53].

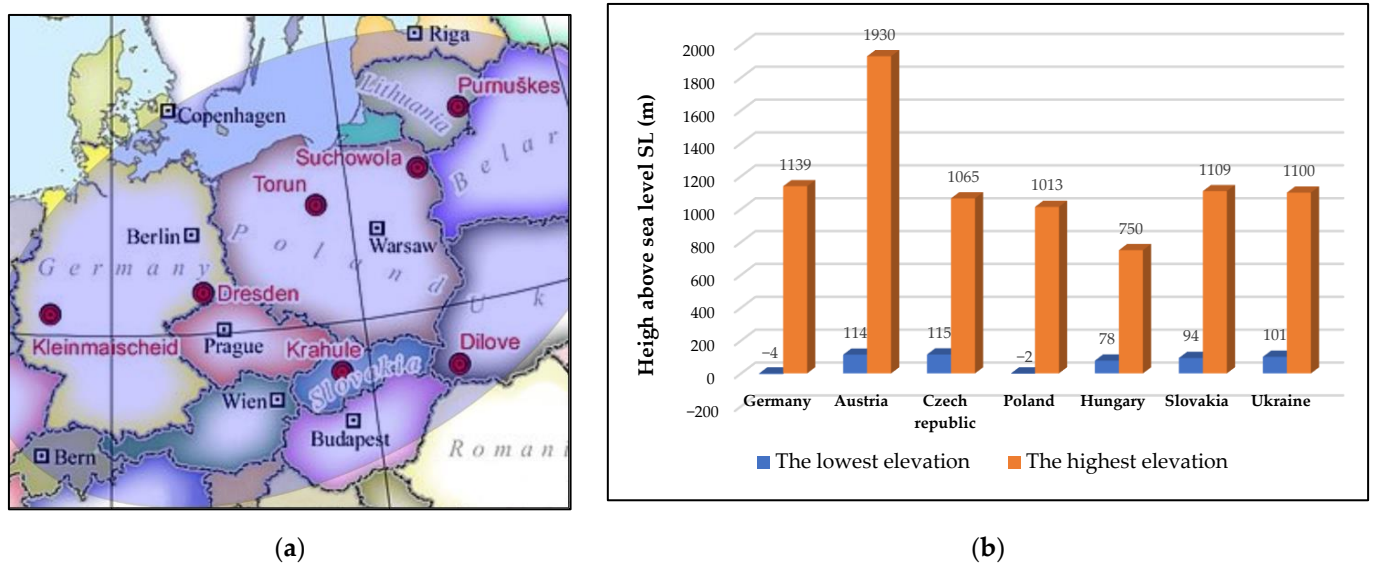


Figure 2. (a) The red dots on the map [56] indicate some of the cities contending for the title Center of Europe: Dilove (Rakhiv, Ukraine), Krahule (or Kremnicke Bane, Slovakia), Dresden and Kleinmaischeid (Germany), Torun and Suchowola (Poland), Bernotai, or Purnuskes (Lithuania), (b) the highest and lowest permanently inhabited municipalities, or places with the lowest altitude of the countries under consideration.

In this article, the highest and lowest permanently inhabited municipalities, or places with the lowest altitude of the countries under consideration are presented. The altitude is related to the definition point of the municipality, which means the center of gravity of the settlement of the town for each country was determined (Figure 2b): Germany: Neuen-dorf-Sachsenbande (4 m b.s.l.-meters below sea level)-Oberjoch (1139 m a.s.l.-meters above sea level), Austria: National Park Neusiedler See-Seewink (114 m a.s.l.)-Ober-gurgl-Hochgurgl (1930 m a.s.l.), the Czech Republic: Hrensko na Decinsku (115 m a.s.l.)-Kvilda (1065 m a.s.l.), Poland: Marzecino (2 m b.s.l.)-Ząb (1013 m a.s.l.), Hungary: Tisza (78 m a.s.l.)-Matraszentimre (750 m a.s.l.), Slovakia: Klin nad Bodrogom (94 m a.s.l.)-Demanovská Dolina (1109 m a.s.l.), Ukraine: Ruski Heivtsi (101 m a.s.l.)-Vypchyna (100 m a.s.l.).

2.2. Basic Criteria for the Structural Pavement Design Assessment

When designing the roadways of land roads in the Slovak Republic, there are decisive codified provisions in the road Act No. 135/1961 Coll. [39]. It is stated that the design of land roads is carried out according to the valid Slovak technical standards, technical regulations, and objectively determined results of research and development for road infrastructure. The correctness of the design of the pavement structure with its degree of reliability for the entire design period is assessed using criteria. The design of the pavement structure must meet the basic requirements criteria, which are:

- A. Road protection against the adverse effects of subsoil freezing;
- B. Ratio of flexure tensile strength and critical bending stress in asphalt or cement-bound pavements layers.

The design of the pavement structure according to criterion A. is satisfactory when the real thermal resistance of the pavement R_r ($\text{m}^2 \cdot \text{K} \cdot \text{W}^{-1}$) is equal to or greater than the necessary thermal resistance of the R_n ($\text{m}^2 \cdot \text{K} \cdot \text{W}^{-1}$) determined based on the requirement to not allow greater freezing of the soil in the subsoil than is allowed. The condition for n

pavement construction layers with thickness h_i (m) and thermal conductivity coefficient λ_i ($\text{W}\cdot\text{m}^{-1}\cdot\text{K}^{-1}$) is expressed by the formula:

$$\sum_{i=1}^n \frac{h_i}{\lambda_i} \geq 0.102 \cdot FI_n^{0.3} + \frac{h_{pf}}{\lambda_{ss}} \quad (1)$$

	FI_n	frost index determined for the respective periodicity n	(°C)
where:	h_{pf}	permissible thickness of pavement freezing	(m)
	λ	thermal conductivity coefficient of subgrade soil.	($\text{W}\cdot\text{m}^{-1}\cdot\text{K}^{-1}$)

Criterion B. for the assessment of mechanical efficiency of asphalt pavements is described in detail in [17,18] and CCP in [57,58]. According to [39], implemented through TP 098, the structural safety design of cement concrete (CC) cover must satisfy the condition that the maximum flexural tensile stress from a single load and repeated loads on the longitudinal or transverse joint of the CC plate must be greater or equal than to the flexural tensile strength of the cement concrete at the specified utilization factor. When calculating the stresses in the CC plate, the joint effect of stresses from traffic and thermal stress is assessed. According to TP 098 for the pre-assessment of CCP can be used modified Westergaard equations, the rigid plate calculation on elastic multi-layered half-space, Pickett, and Ray influence surfaces, and for the final assessment it is necessary to use FEM calculation. The method of thermal stress calculation is detailed in [57], where the research results presented in the Conclusions of this article are presented.

2.3. Dependence of Climatic Characteristics of Central Europe on Altitude

To design pavements, the following climatic characteristics are used in Slovak Republic conditions:

- Average annual air temperature-design of concrete pavements;
- Frost index (FI)-design of asphalt and concrete pavements.

These characteristics are obtained by evaluating air temperature measurements. According to international conventions, this temperature is measured at a height of 2.0 m above terrain at 7 a.m., 2 p.m., and 9 p.m. during the day. For practice, the daily temperature flow is expressed by average daily air temperature T_s , which is calculated as:

$$T_s = (T_7 + T_{14} + 2 \cdot T_{21}) / 4. \quad (2)$$

The average annual air temperature T_a (°C) is expressed by the following formula:

$$T_a = \sum_{i=1}^{365} T_{s,i} / 365. \quad (3)$$

In Slovakia, the civil engineering design value T_a is determined from long-term measurements of air temperatures (Figure 3, selected meteorological stations in Slovakia), for pavement engineering purposes is used the average annual temperature map according to STN 73 6114 [59] or objectified research results.

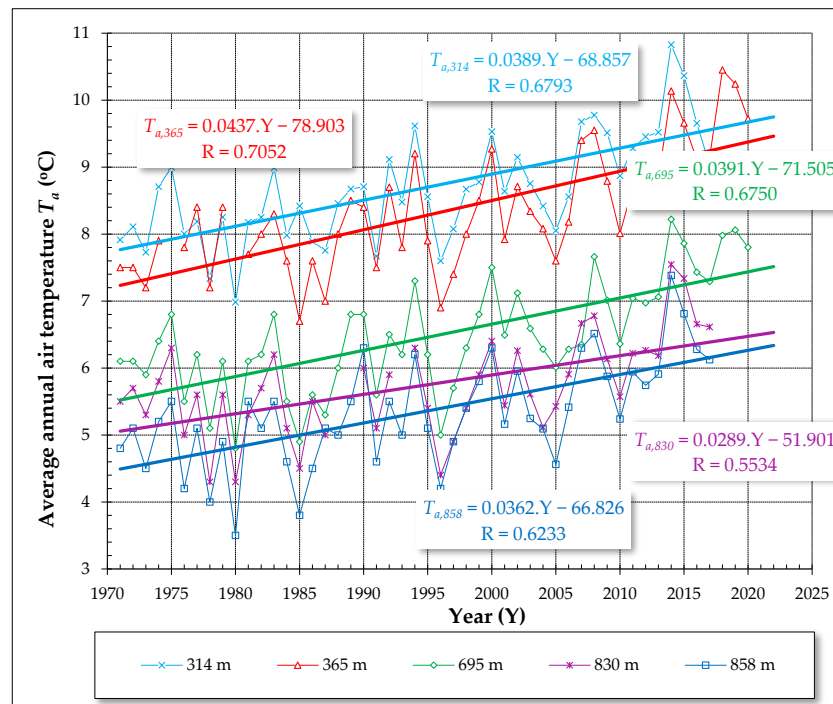


Figure 3. Correlation dependencies of the evolution of annual average temperatures for altitudes 314, 365, 695, 830, and 858 m a.s.l. for the period 1971 to 2020.

The following equations for the computing of T_a were objectified for the SL above 300 m and individually evaluated time periods A (Figure 4):

- Average annual temperature 1971–2000;

$$T_{a,1971-2000} = -0.00574 \cdot SL + 10.06 \tag{4}$$

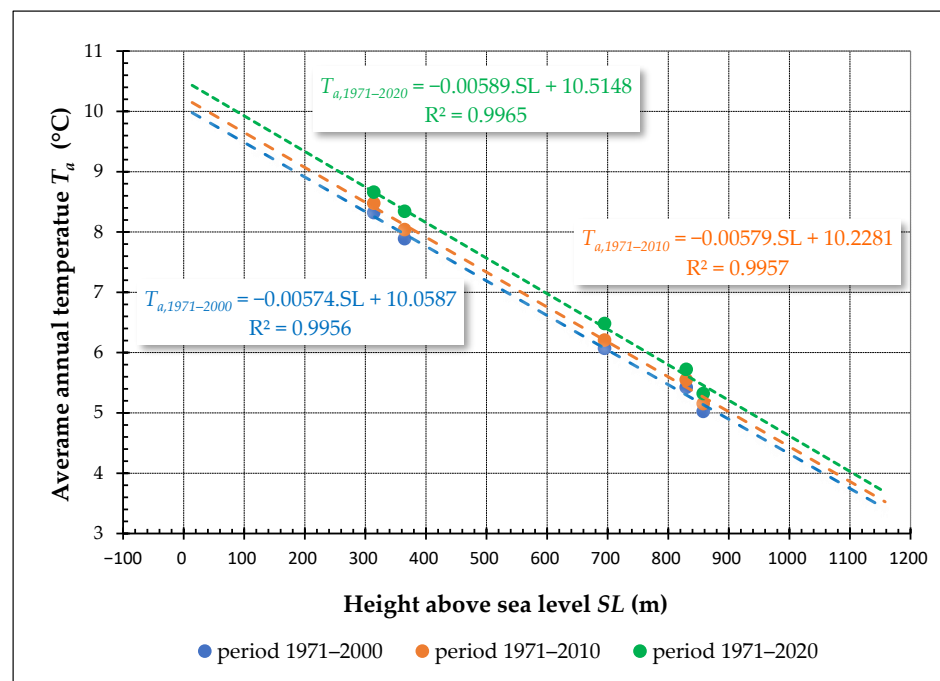


Figure 4. Dependence of the average annual air temperature of Central Europe for the period 1971–2000, 1971–2010, and 1971–2020 exceeding 300 m above sea level.

- Average annual temperature 1971–2010;

$$T_{a,1971-2010} = -0.00579 \cdot SL + 10.23 \quad (5)$$

- Average annual temperature 1971–2020;

$$T_{a,1971-2020} = -0.00589 \cdot SL + 10.51. \quad (6)$$

In a scientific monograph [60] and contributions [18,38] was presented the correlation of frost indexes FI (as the sum of the negative average daily air temperatures consecutive in winter) dependence on the altitude of specific meteorological stations of Slovakia, starting from the logical premise of frost index dependence on altitude (SL).

The equations presented in Figure 5 express the dependence of the computing frost indexes of FI_n (for different periodicity n of 0.10, 0.15, and 0.25) which were objectified for the SL above 300 m and individually evaluated time periods.

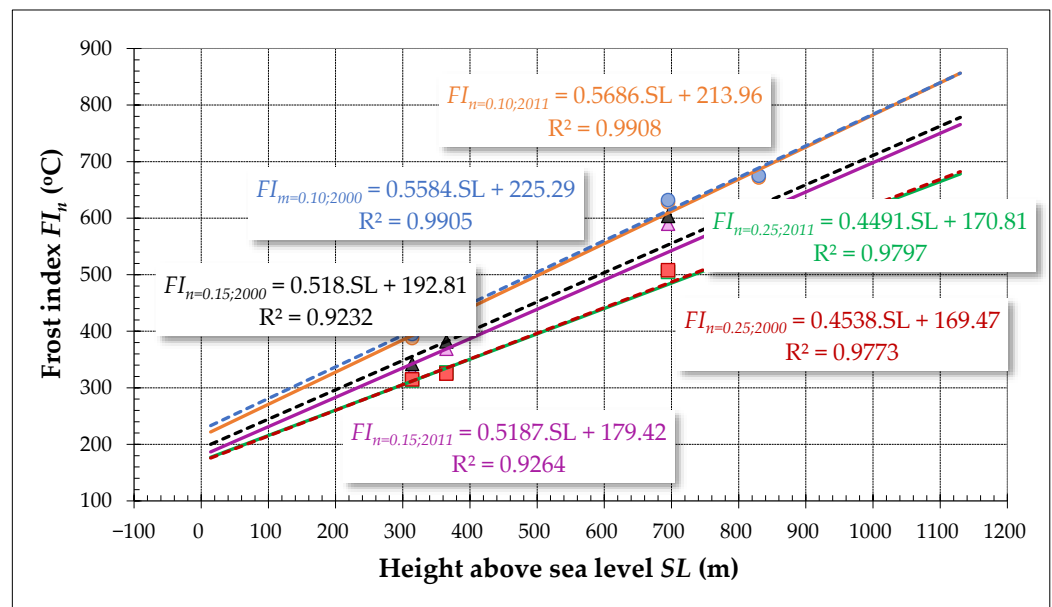


Figure 5. Objectified correlation dependences of the Slovak design values of the frost index FI_n for the periodicity 0.10, 0.15, 0.25 on the altitude SL for the period 1971 to 2000 and 1971 to 2011.

The authors conducted separate evaluations of the dependence of frost indices on the elevation of the pavement of interest for the period 1971 to 2000 and the period 1971 to 2011. By comparing the objectified FI_n dependencies for all periodicities (n of 0.10, 0.15, 0.25), an average level of 98.4% of the RI values determined for the period 1971 to 2000 was obtained for the period 1971 to 2011 evaluated. This represents a 1.6% reduction in FI when considering the average values for the 40 years (1971–2011) and the 30 years from 1971 to 2000.

2.4. Flexural Strength of Isomorphic Models of Foam Concrete FC 500 Construction Layer

Two isomorphic models of base systems for traffic structures with a base layer of foam concrete were built at the authors' workplace, namely the model of FC 500 base layer and the model with FC 500 base layer with a reinforcing basalt mesh ORLITECH® Mesh (OM). In previous work by the authors [48–50], the possibility of using composite models of foam concrete with nonwoven PP (polypropylene) geotextile $200 \text{ g} \cdot \text{m}^{-2}$ (Filtek); geogrid with nonwoven PP fibers $60 \text{ g} \cdot \text{m}^{-2}$, and PET (polyethylene terephthalate) mesh (Armatex); and geogrid made of stretched monolithic flat bars and filter geotextile (Combigrid) have been verified in situ and in the lab. The best result was obtained with the nonwoven polypropylene geotextile material, which was used for the applications reported in this paper.

The basalt (composite) reinforcing mesh was chosen as the optimal replacement for steel reinforcement for its advantages such as lack of corrosion compared to steel mesh, lower weight (density of $360 \text{ g}\cdot\text{m}^{-2}$), higher tensile strength (1284 to 1458 MPa), better cohesion with concrete, lower thermal expansion (thermal coefficient of linear expansion of $6 \text{ to } 10 \times 10^{-6} \text{ }^\circ\text{C}^{-1}$), fewer cracks in concrete, thermal and electrical insulator, as well as easy handling and installation. The composite mesh used consisted of bars in thickness of 3 mm in diameter and $100 \times 100 \text{ mm}$ mesh size, in 2 perpendicular directions connected by special material. The application of OM is also very advantageous in marine environments such as harbors, piers, and dikes and in structures that need electromagnetic neutrality such as hospitals. The measurements of foam concrete models were performed in-situ and were complemented by laboratory measurements of mechanical characteristics.

Under laboratory conditions, flexural strength was determined as a material characteristic that is the critical property of FC in terms of reaching the limit state of pavement use and is input into the design and assessment calculations of pavements of engineering structures. The strength was calculated for test specimen FC 500 without geotextile, FC 500 with standard nonwoven PP geotextile GTX $200 \text{ g}\cdot\text{m}^{-2}$, and FC 500 with GTX 200 with basalt mesh. The test specimen was a prism-shaped beam ($100 \times 100 \times 400 \text{ mm}$) in accordance with STN EN 12390-5:2020 [61] and the set contained a total of 49 specimens. The flexural strength f_{cf} of the test specimen was determined by applying a symmetrical two-point method of loading at a constant loading rate on a servo-controlled testing device [61]. As the specimens were subjected to bending, the maximum load was recorded once the tensile stresses exceeded the flexural strength of the FC and cracks started to occur when the bending moment was reached (Figure 6).

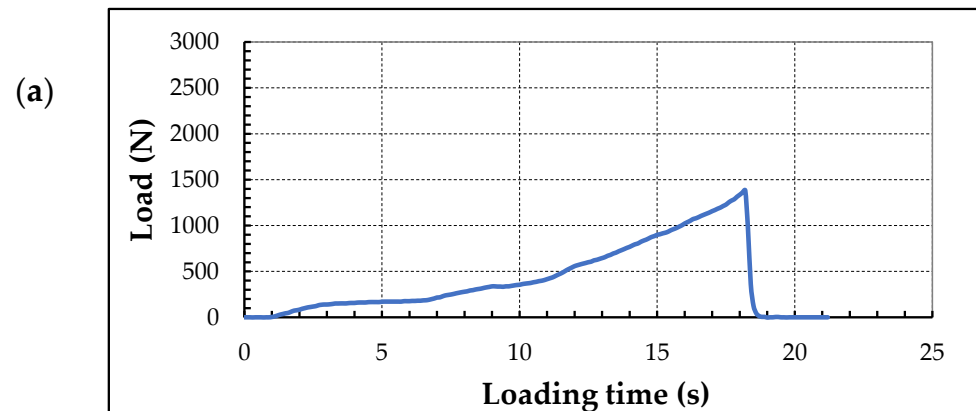


Figure 6. Cont.

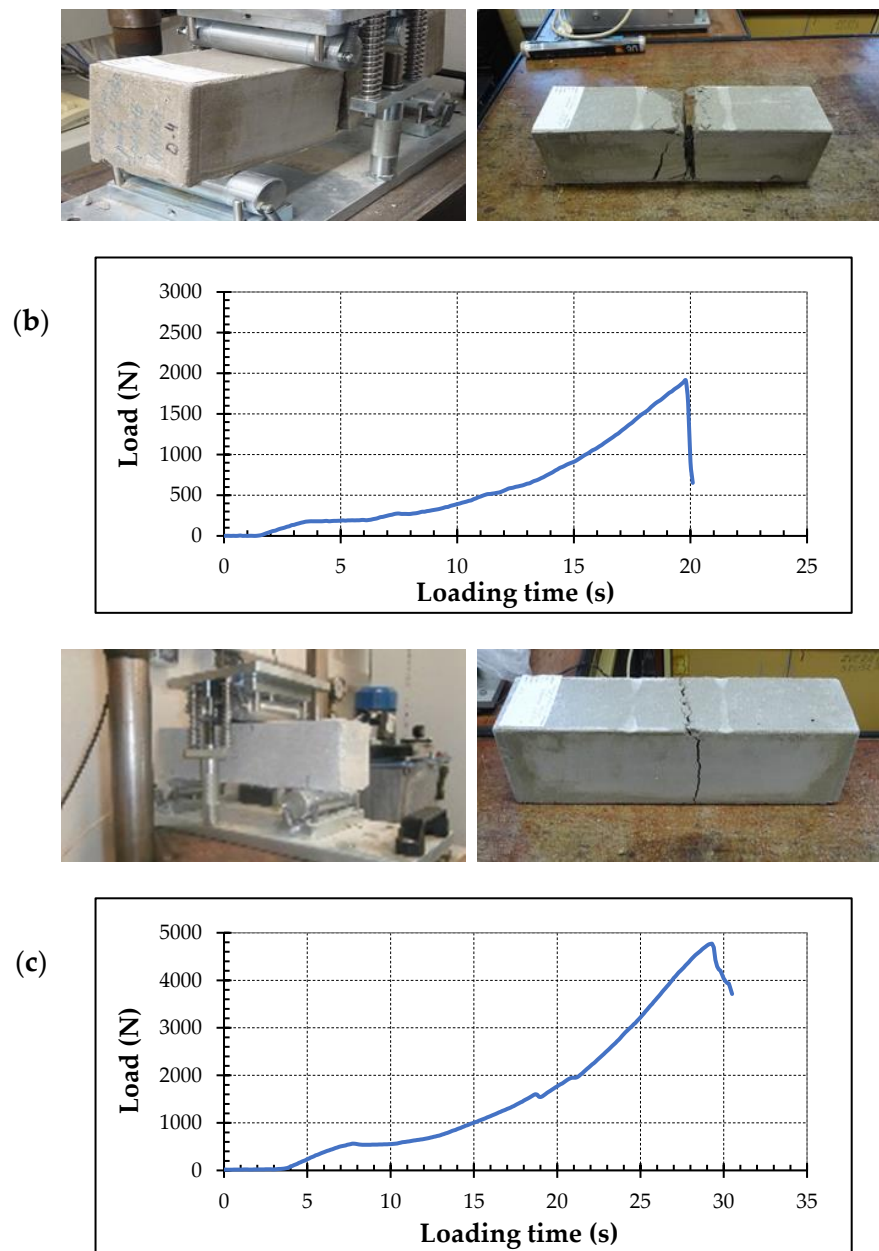


Figure 6. Test samples and examples of record of the test; (a) foam concrete FC 500, (b) foam concrete FC 500 + GTX 200, and (c) foam concrete FC 500 + GTX 200 + OM.

The Grubbs test and Dixon's critical values test were used to remove outliers in the set of measurements. The measured flexural strength of the tested specimen after removing outliers is shown in Table 1 and Figure 7. Before the determination of flexural strength, the measurement of density on compaction of the foam concrete was performed (Table 1). The results showed that the use of basalt mesh will significantly increase the flexural strength of foam concrete, as compared to hydraulically cement bound granular mixture CBGM with strength classification $C_{5/6}$ and design value of flexural strength 0.50 MPa which is standardly used in a base layer of pavements. A similar increase in flexural strength can be achieved by using fibers in foam concrete, which has been demonstrated by many measurements [27,34]. To determine the design values of the foam concrete characteristics, the lower limit of the mean value interval at a 95% confidence level was used as input data for the three-dimensional modeling of pavement with a layer of foam concrete.

Table 1. Flexural strength and density of tested FC specimens.

	Density Average Value (kg·m ⁻³)	Flexural Strength (N·mm ⁻²)			Design Value
		Average Value	Standard Dev.	Student's Distribution t _{0.05}	
FC 500	522	0.376	0.055	2.080	0.36
FC 500 + GTX 200	516	0.521	0.086	2.069	0.48
FC 500 + GTX 200 + OM	525	1.370	0.165	4.303	0.96

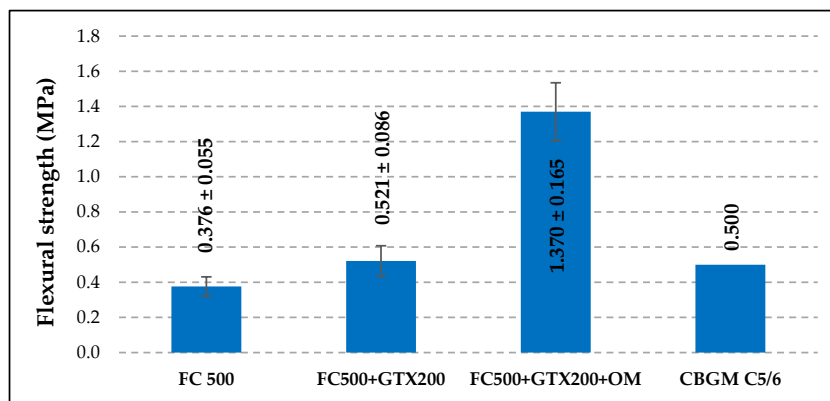


Figure 7. Results of flexural strength of tested foam concrete samples tested.

The isomorphic models of the base systems of the traffic structures were built on a uniform subbase formed by anthropogenesis soil of intermediate-plastic clay of rigid consistency (Proctor compaction test, optimum water content 15.8% and bulk density 1632 kg·m⁻³), which is often found in the territory of the Slovak Republic. The bearing capacity determined by a static load test was determined to be 15.0 MPa.

To determine the properties of different load-bearing bases, both composite models were built on two different sub-base layers. The first sub-base layer was constructed of coarse aggregate 8/16 mm in 150 mm thickness separated from the subgrade by a separating geotextile. The bearing capacity of the sub-base layer was 19.6 MPa (Figure 8). The second sub-base structure was constructed of a 350 mm thick coarse aggregate layer on the subgrade using a separation geotextile with a bearing capacity of 33.3 MPa after compaction. Two isomorphic models of the base system from foam concrete FC 500 with GTX 200 and composite FC 500 with GTX 200 reinforced by basalt mesh in 220 mm thickness were made on both sub-base constructions (Figure 9).

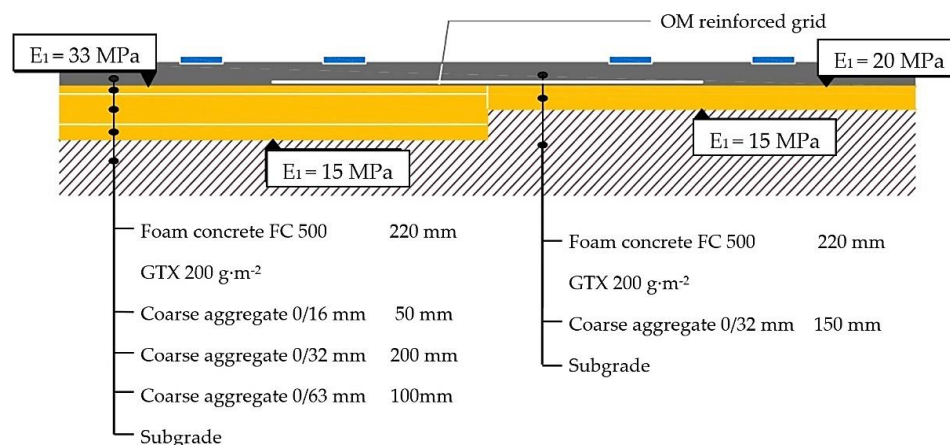


Figure 8. Isomorphic models of base construction.

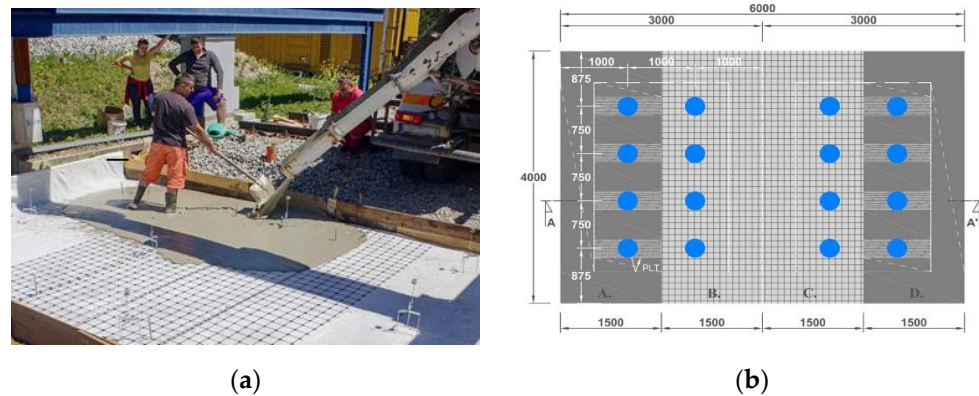


Figure 9. (a) Construction of experimental isomorphic models, (b) scheme of measuring points.

The maximum contact stress of loading by the static load test was chosen to be $0.6 \text{ MN}\cdot\text{m}^{-2}$ corresponding to the design vehicle axle parameter with a mass of 10 tones. The achieved load-bearing capacity values expressed by the modulus of elasticity from the second loading cycle E_e are shown in Table 2, from which the modulus of elasticity of the base layer from foam concrete (FC 500 and FC 500 + OM) was subsequently determined by back-calculation from the measured values of the equivalent modulus of elasticity on the surface of subgrade and the sub-base layer and known thicknesses (Table 2). Similar to the results of the laboratory measurements (Table 1), the in-situ measurements showed that reinforcing the foam concrete with basalt mesh will increase the modulus of elasticity of the foam concrete layer. The results obtained are comparable to the values found by [62,63] where for foam concrete densities of 500 to $1600 \text{ kg}\cdot\text{m}^{-3}$ the values of the modulus of elasticity are in the range of 1 to $12 \text{ kN}\cdot\text{mm}^{-2}$.

Table 2. Results of the modulus of elasticity.

Isomorphic Model	Modulus of Elasticity (MPa)		
	Sub-Base	Equivalent Modulus E_e	Back-Calculation E
FC 500 + GTX 200	19.6	82.50	1412.5
	33.3	130.75	2062.5
FC 500 + GTX 200 + OM	19.6	107.75	3675.0
	33.3	155.00	3575.0

3. Three-Dimensional Model of a Cycle Pavement with a Layer of FC Reinforced with a Basalt Mesh

The design of the pavement system is influenced by axle loads, axle configuration, tire contact patches, number of load cycles, vehicle speed, and the effect of temperature changes on the pavement or area declination. Understanding the constitutive relationship between stress and strain in FEM is more than necessary. This is due to the use of stress-strain analysis to predict pavement failures. Thus, the relative conditions of different layers in the pavement structure can also be analyzed. Some basic issues about pavement performance can be best answered by three-dimensional finite element analysis tools. However, the processing and time required to model pavements accurately make these analyses difficult to use [64]. The traffic means (vehicles) are considered as static load. Dynamic load is still the subject of research.

In accordance with the Road Act No. 135/1961 [39], when assessing the final design of a cement concrete pavement (CCP), stresses must be evaluated using FEM based on the limit axle load $2P = 115 \text{ kN}$, in accordance with the requirements of TP 098 [58]. FEM is a universal and very efficient numerical method for solving continuum mechanics problems. In general, it involves dividing the solved continuum surface into a system of small finite elements, connected at the nodes of the mesh. The generated discrete system must satisfy

the continuity and the balance conditions. The created model can be made of 1D, 2D, and 3D elements, each element of which is described by a system of algebraic equations.

In the case of the computational model of the cycle pavement (Pavement 3) with a layer of foam concrete (FC 500) reinforced with a basalt mesh-ORLITECH composite system (OM), it is a surface stress solution. It is a complicated model created from 3D elements in VisualFEA (8 node quadrilateral) providing all the necessary information about the stiffness element, which it includes in the elements of the stiffness matrix. The finite elements used and the process of creating the 3D model is shown in Figure 10.

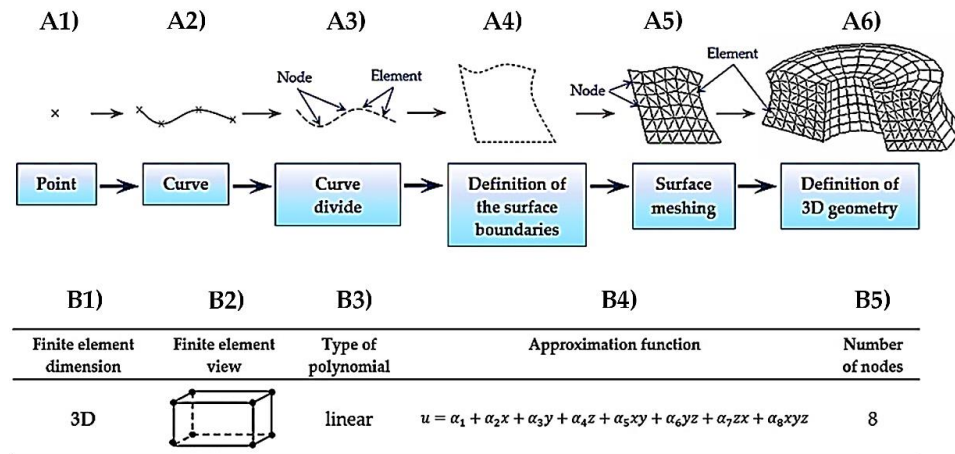


Figure 10. Finite elements used in modeling and the process of creating a 3D model; (A1)—definition of basic points of model shape; (A2)—connecting basic points using lines and curves (thread model simplified); (A3)—dividing lines and curves (setting boundaries for elements); (A4)—definition which lines creates boundaries for element meshing procedure (surface mesh); (A5)—meshing of defined surfaces with 2D element types (not assigned width); (A6)—from defined surface boundaries creating of volume element mesh (or other advanced methods can be used); (B1)—real dimension of element used for pavement layer; (B2)—hexahedron type of volume element used for model; (B3)—type of polynomial interpolation for used element; (B4)—mathematical expression of approximation function for FEM solution; (B5)—number of element nodes for solving of displacement (define the difficulty of computation).

The layers of the numerical model of the cycle pavement and the mechanical characteristics used are shown in Table 3 (Pavement 3).

Table 3. Cycle pavement construction and characteristics of layers.

Cycle Pavement Construction	Thickness (mm)	Modulus of Elasticity (MPa)			Poisson’s Ratio (MPa)			Flexural Tensile Strength (MPa)		
		0 °C	11 °C	27 °C	0 °C	11 °C	27 °C	0 °C	11 °C	27 °C
		Single-layer cement concrete pavement	180	35.10 ³			0.2			4.0
CC III; PE (polyethylene) geotextile										
Foam concrete with reinforcing mesh	100	1800			0.23			1.0		
FC 500 + OM, base layer										
Gravel crushed stone										
Unbound gravel materials (UGM), sub-base layer	150	350			0.3			-		

The influence of the layers (except the stiffest layer), including the subgrade, is included by a linearized calculation in the Spring constant per unit area Δz of the 3D element. In this case, the value of $\Delta z = 34.34 \text{ MN}\cdot\text{m}/\text{m}^2$ is obtained by substituting the modulus of elasticity

of the subgrade $E = 30$ MPa, the effective width of the contact area of the rigid elements with the elastic subgrade $B = 0.96$ m, and the Poisson number $\nu = 0.3$ into relation (7).

$$\Delta_z = E / \left[B \cdot (1 - \nu^2) \right] \quad (7)$$

The contact between the main layers (CC III and FC 500 + OM) had to be solved by using a special tool of VisualFEA-Volume Interface, which can reduce the perfectly rigid interaction of the layers on the contact surfaces. The influence of the PE separation geotextile is thus considered. The reinforcing 1D elements of the basalt mesh are modeled using the Embedded Bar function and the results from the simplified model are shown in Figure 11. Future work will continue to refine the 3D model and experimental measurements will be processed to calibrate and verify the developed model.

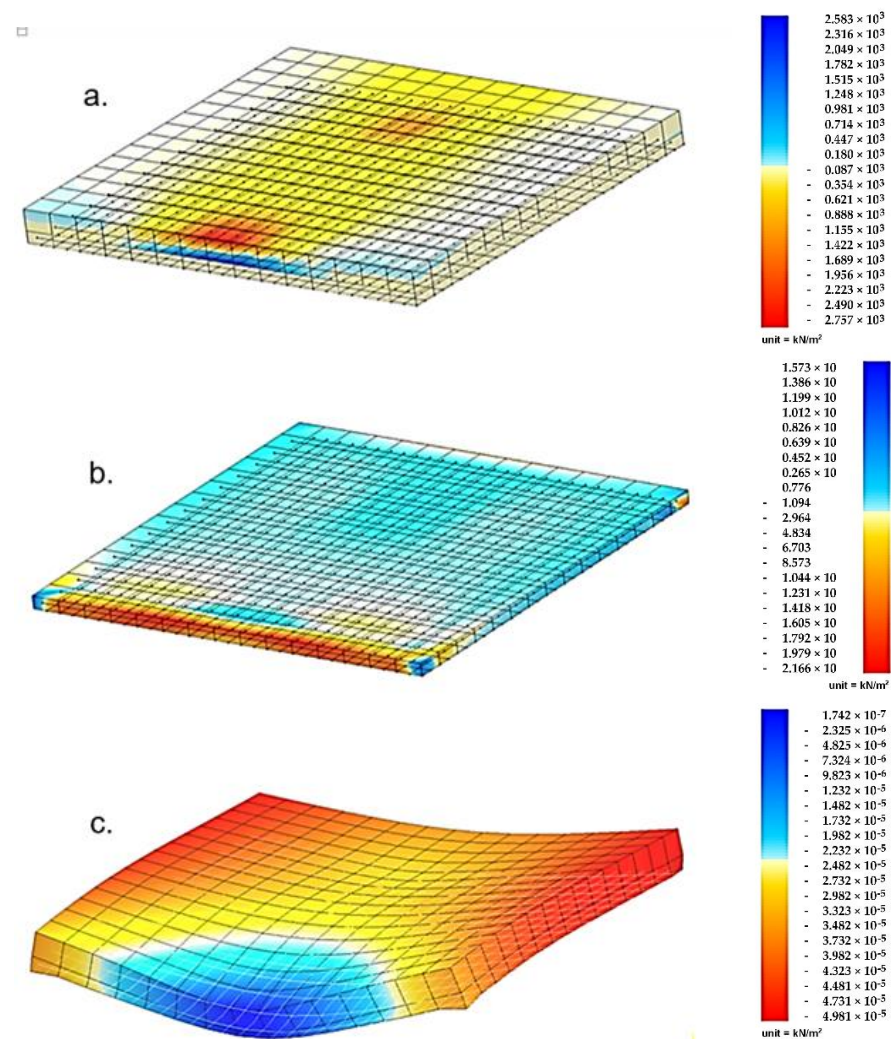


Figure 11. Skin stress and strain on the FEM model, (a) maximum normal stresses on the model σ_x , (b) maximum normal stresses σ_x on the 3D foam concrete solid, (c) maximum displacement from the 2P load.

A numerical model of the pavement was created from the solid elements. In this model, it is possible to track not only the stresses on the surfaces (skin stresses) but also the changes along with the height of the solid.

The plate models do not allow this option (Figure 11a). Another option is to turn off the particular level at which the pavement layers are modeled. It is then possible to watch the effect of the load, for example on a layer of foam concrete (Figure 11b). The

maximum deformation in the vertical direction due to load as required by TP 098 is shown in (Figure 11c).

Because dimensional stresses are solved, it is also possible to obtain from the model the contact stresses arising between the modeled parts. According to TP 098 for the pre-design of dimensions and design assessment in the project documentation for the construction plan or planning permission, the modified equations can also be used. These are the Westergaard equations (WEST), the rigid plate calculation on elastic multilayered half-space (LAYMED) or the Pickett and Ray influence surfaces (PICRA), and Table 4 shows the stresses obtained by these methods.

Table 4. Stresses results obtained by different methods.

Numerical Results-Stresses (Obtained by Different Methods)	Model of Cycle Pavement 3	Single Load
Westergaard	(WEST)	3.113 MPa
Pickett and Ray	(PICRA)	3.298 MPa
Elastic multilayered half-space	(LAYMED)	2.965 MPa
Finite element method	(FEM)	2.583 MPa
Thermal Stresses	(THERM)	1.083 MPa
Criteria Limit value according to standard TP 098	CC III	4.0 MPa

The authors addressed the method of determining thermal stresses in road constructions in the following scientific paper. Decky, M., Papanova, Z., Juhas, M., and Kudelcikova, M. (2022). Evaluation of the Effect of Average Annual Temperatures in Slovakia between 1971 and 2020 on Stresses in Rigid Pavements. *Land*, 11(6), 764 [57]. One of the main conclusions [57] is that using composite foam concrete is most appropriate in terms of mitigating the effects of temperature on cement concrete pavements, especially on jointed plain concrete pavements and jointed reinforced concrete pavements.

4. Discussion

The current civil engineering industry is a dominant contributor to carbon dioxide emission [65] and therefore is necessary to reduce it through the circular economy pavement circular economy (PCE). Generally, CE is perceived as an industrial economy that is restorative or regenerative by intention and which aims to keep products, components, and materials at their highest utility and value, all the time [66–68]. It is necessary to try to choose more environmentally friendly variants of construction projects, and use a more environmentally friendly material, which has a higher degree of recyclability and reusability [69,70]. The European experts in the field of PCE ascribe the highest importance to the high durability of asphalt and cement concrete pavements (perpetual), special innovative material design to meet climatic requirements, and wider usage of recyclable materials [70–72]. A recent increase in the use of ecofriendly, natural fibers as reinforcement for the fabrication of lightweight, low-cost polymer composites can be seen globally. One such material of interest currently being extensively used is basalt fiber, which is cost-effective and offers exceptional properties over glass fibers [73]. Despite the many benefits of using basalt fiber in concrete, only a restricted number of research has been found in the literature concerning basalt fiber or mesh reinforced construction layer of pavements [74–77]. The authors' long-term research of climatic changes of CE [17–19,57,60] and research in the field of applicability of foam concrete with a bulk density of $500 \text{ kg}\cdot\text{m}^{-3}$ in transport constructions [48–50] created credibility conditions for the design cycle pavements using composite foam concrete (CFC) with basalt mesh at high altitudes of CE. In the area of increasing the mechanical efficiency of the road, the increase in the tensile strength of CFC from 0.5 MPa to 1.3 MPa was objectified due to the use of a basalt reinforcement net. To provide credible design and assessment of such pavements through validated FEM models, they present

the results of research on climatic characteristics for the period 1971–2020, according to the World Meteorological Organization, the weather trends for the last 30 years are assessed.

As part of their research, the authors objectified the correlation dependences of average annual temperatures and frost index from the altitudes of Central Europe exceeding 300 m above sea level (Figures 4 and 5). The following results from Figure 4 determine the evaluated time intervals and the considered altitudes of 300 and 1100 m above sea level are:

- Average annual temperature 1971–2000 8.34 °C (300 m) and 3.75 °C (1100 m);
- Average annual temperature 1971–2010 8.49 °C (300 m) and 3.86 °C (1100 m);
- Average annual temperature 1971–2020 8.75 °C (300 m) and 4.03 °C (1100 m).

Due to increasing air temperatures, the frost index decreases and for the above range of altitudes, the authors found:

- Average value of the frost index in the period 1971–2000 for:
n = 0.10 392.8 (300 m) and 839.5 (1100 m);
n = 0.15 348.2 (300 m) and 762.6 (1100 m);
n = 0.25 305.6 (300 m) and 668.7 (1100 m);
- Average value of the frost index in the period 1971–2011 for:
n = 0.10 384.5 (300 m) and 839.4 (1100 m);
n = 0.15 335.0 (300 m) and 750.0 (1100 m);
n = 0.25 305.5 (300 m) and 664.8 (1100 m).

Using the presented research results, which resulted in the granting of Slovak patents for the described CFC structural layer, the following structural composition of the cycle pavements was optimized. For the possibility of mutual comparison and interchangeability of the pavement, covers were designed rigid (1–3), semi-rigid (4 and 5) pavements, whereas pavement 3 and 5 has innovative base courses CFC from foam concrete FC 500 reinforced by basalt mesh.

The results in Table 5 show the possibilities of reducing the overall pavement thickness by 40 mm for the rigid pavement with a cement concrete surface and by 100 mm for the semi-rigid pavement with an asphalt surface. In continuing the research, the authors want to focus on further saving non-renewable natural resources and assessing of life cycle cost of CFC and their environmental impact.

Table 5. The overview of thickness (mm) cycle pavement construction layers of Pavements 1 to 5.

Pavement Construction Layer	Pavement 1	Pavement 2	Pavement 3	Pavement 4	Pavement 5
Cement concrete for surface CC III; EN 13877	190	190	180	-	-
Asphalt concrete for base course AC 11; EN 13108-1	40	-	-	-	-
Asphalt concrete for wearing course AC 8; EN 13108-1	-	-	-	30	30
Asphalt concrete for binder course AC 16; EN 13108-1	-	-	-	50	50
Asphalt concrete for road base AC 16; EN 13108-1	-	-	-	50	50
Cement bound granular mixture CBGM C _{5/6} ; EN 14227-1	150	-	-	150	-
Foam concrete + reinforcing basalt mesh FC 500 + OM	-	-	100	-	100
Unbound mixtures (UM) for sub-base layer UM 0/31.5; EN 13285	-	180	-	-	-
Unbound mixtures (UM), for sub-base layer UM 0/31.5; EN 13285	180	180	150	200	150
Elasticity modulus of subgrade <i>E</i> (MPa)			min. 30		
Pavement service life (years)			min. 30		
Total pavement thickness (mm)	560	550	430	480	380
The required thermal resistance of the pavement (m ² ·K·W ⁻¹)		0.260 for altitude 300 m according to TP 098 [58] 0.412 for altitude 1100 m according to TP 098 [58]			
The real thermal resistance of the pavement (m ² ·K·W ⁻¹)	0.263	0.285	0.650	0.286	0.676

5. Conclusions

With the increase in global warming, the construction sector [17,18,57] is trying to find an alternative to ordinary concrete and presently the emerging trend is the use of foamed concrete, which is a lightweight concrete having a greater strength-to-weight ratio with density varying from 300 to 1800 kg·m⁻³ [33,63]. To use in the base layers of road structures, the need to increase its tensile strength in bending was identified [27,62]. The authors have been intensively addressing these research issues for the last 10 years [48,49] and in this article, they present the application of composite concrete with a bulk density of 500 kg·m⁻³, reinforced with a basalt mesh [50].

The authors present an optimized pavement design of bicycle paths with base layers made of composite foam concrete. First, it was necessary to develop a reliable method for determining the climatic characteristics of Central Europe (CE), specifically the average annual temperature T_a and the frost index (FI). For CE altitudes from 300 to 1100 m and the evaluated period 1971–2020, the temperature range is 8.8 to 4.0 °C. To illustrate the significant effect of T_a on thermal stresses (TS) of cement concrete plates, we give corresponding numerical values for its thickness of 20 cm and dimensions of CC plates 4 × 4 m for temperatures $T_a = 4.5$ and 11.5 °C and modulus of reaction k [57]:

- $k = 100 \text{ MN}\cdot\text{m}^{-3}$ $\text{TS}_{4.5} = 2.26 \text{ MPa}$ $\text{TS}_{11.5} = 1.64 \text{ MPa}$;
- $k = 200 \text{ MN}\cdot\text{m}^{-3}$ $\text{TS}_{4.5} = 2.63 \text{ MPa}$ $\text{TS}_{11.5} = 1.91 \text{ MPa}$;
- $k = 300 \text{ MN}\cdot\text{m}^{-3}$ $\text{TS}_{4.5} = 2.72 \text{ MPa}$ $\text{TS}_{11.5} = 1.92 \text{ MPa}$.

For the evaluated period 1971–2011 and periodicity $n = 0.10, 0.15, 0.25$, this range is from $Fin = 385, 335, 306$ °C to 839, 750, 665 °C. The evaluation from the point of view of the design of the road confirmed for Central Europe a significant increase in temperatures over the last 10 years and a very slight decrease in frost indices.

When assessing the mechanical efficiency of pavement construction, the decisive characteristic is the flexural strength of the subbase layers. Through extensive experiments on homomorphic [20,78] and isomorphic models [49,79] of pavement layers, the authors objectified the following research results. For foam concrete with a volume weight of 500 kg·m⁻³ (FC 500) with the use of geotextile (GTX) and reinforcing basalt Orlichtech mesh (OM), the following average flexural strengths were objectified: FC 500 = 0.38 MPa, FC 500 + GTX = 0.52 MPa, FC 500 + GTX + OM = 1.37 MPa.

The determined strengths are comparable to the standard subbase material as CBGM (Cement Bound Granular Mixture) with strength classification C_{5/6}, C_{8/10}, and C_{12/15}, which have design values of flexural strength of 0.50, 0.80, and 1.00 MPa [59].

The presented research results made it possible to reduce the total thickness of cement concrete cycling pavements (CCCP) from 56 to 43 cm and flexible (asphalt) concrete from 48 to 38 cm for the high altitudes of Central Europe (Table 5). The validated FEM model is required for final assessments of rigid pavements by the requirements of Act No. 135/1961, Act on Roads [39] implemented to pavement design through TP 098 [58].

Author Contributions: Conceptualization, M.D.; Formal analysis, Z.P.; Investigation, E.R.; Methodology, E.R.; Software, Z.P.; Supervision, M.D.; Visualization, K.H.; Writing—original draft, M.D., K.H., Z.P. and E.R. All authors have read and agreed to the published version of the manuscript.

Funding: This research was funded by Ministry of Education, Science, Research and Sport of the Slovak Republic, grant number KEGA:027ŽU-4/2022.

Institutional Review Board Statement: Not applicable.

Informed Consent Statement: Not applicable.

Data Availability Statement: Not applicable.

Conflicts of Interest: The authors declare no conflict of interest.

References

1. Ruiz-Mallén, I.; Heras, M. What Sustainability? Higher Education Institutions' Pathways to Reach the Agenda 2030 Goals. *Sustainability* **2020**, *12*, 1290. [CrossRef]
2. Dodds, F.; Donoghue, A.D.; Roesch, J.L. *Negotiating the Sustainable Development Goals: A Transformational Agenda for an Insecure World*, 1st ed.; Routledge: Abingdon-on-Thames, UK, 2016; ISBN 978-1138695085.
3. Colglazier, W. Sustainable Development Agenda: 2030. *Science* **2015**, *349*, 1048–1050. [CrossRef] [PubMed]
4. Švajlenka, J.; Kozlovská, M. Modern Method of Construction Based on Wood in the Context of Sustainability. *Civ. Eng. Environ. Syst.* **2017**, *34*, 127–143. [CrossRef]
5. Kibert, C.J. Establishing Principles and a Model for Sustainable Construction. In Proceedings of the First International Conference of CIB TG 16 on Sustainable Construction, Tampa, FL, USA, 6–9 November 1994.
6. Vanegas, J.A.; Pearce, A.R. Drivers for Change: An Organizational Perspective on Sustainable Construction. In Proceedings of the Construction Congress VI: Building Together for a Better Tomorrow in an Increasingly Complex World, Orlando, FL, USA, 20–22 February 2000; Volume 278, pp. 406–415.
7. McDonough, W.; Braungart, M. *Cradle to Cradle: Remaking the Way We Make Things*, 1st ed.; North Point Press: Albany, CA, USA, 2002; ISBN 978-0865475878.
8. Pulaski, M.H.; Horman, M.J.; Riley, D.R.; Dahl, P.; Hickey, A.; Lapinski, A.R.; Magent, C.; Shaltes, N. *Field Guide for Sustainable Construction*; The Pennsylvania State University: State College, PA, USA, 2004.
9. Mallick, R.B.; El-Korchi, T. *Pavement Engineering: Principles and Practice*, 1st ed.; CRC Press: Boca Raton, FL, USA, 2008; ISBN 978-1420060294.
10. Jandačka, D.; Ďurčanská, D. Particulate Matter Assessment in the Air Based on the Heavy Metals Presence. *Civil. Environ. Eng.* **2014**, *10*, 26–39. [CrossRef]
11. Drliciak, M.; Celko, J.; Cingel, M.; Jandacka, D. Traffic Volumes as a Modal Split Parameter. *Sustainability* **2020**, *12*, 10252. [CrossRef]
12. Koglin, T.; Rye, T. The Marginalisation of Bicycling in Modernist Urban Transport Planning. *J. Transp. Health* **2014**, *1*, 214–222. [CrossRef]
13. Hunkin, S.; Krell, K. Promoting Active Modes of Transport: A Policy Brief from the Policy Learning Platform on Low-Carbon Economy. *Interreg Europe* 2019. Available online: https://www.interregeurope.eu/sites/default/files/inline/TO4_PolicyBrief_Active_Modes.pdf (accessed on 7 June 2022).
14. Georgiou, A.; Skoufas, A.; Basbas, S. Perceived Pedestrian Level of Service in an Urban Central Network: The Case of a Medium Size Greek City. *Case Stud. Transp. Policy* **2021**, *9*, 889–905. [CrossRef]
15. Mésároš, P.; Spišáková, M.; Mandičák, T.; Čabala, J.; Oravec, M.M. Adaptive Design of Formworks for Building Renovation Considering the Sustainability of Construction in BIM Environment-Case Study. *Sustainability* **2021**, *13*, 799. [CrossRef]
16. Dolnikova, E.; Katunsky, D.; Darula, S. Assessment of Overcast Sky Daylight Conditions in the Premises of Engineering Operations Considering Two Types of Skylights. *Build. Environ.* **2020**, *180*, 106976. [CrossRef]
17. Trojanová, M.; Decký, M.; Remišová, E. The Implication of Climatic Changes to Asphalt Pavement Design. *Procedia Eng.* **2015**, *111*, 770–776. [CrossRef]
18. Remišová, E.; Decký, M.; Podolka, L.; Kováč, M.; Vondráčková, T.; Bartuška, L. Frost Index from Aspect of Design of Pavement Construction in Slovakia. *Procedia Earth Planet. Sci.* **2015**, *15*, 3–10. [CrossRef]
19. Remišová, E.; Decký, M.; Mikolaš, M.; Hájek, M.; Kovalčík, L.; Mečár, M. Design of Road Pavement Using Recycled Aggregate. *IOP Conf. Ser. Earth Environ. Sci.* **2016**, *44*, 022016. [CrossRef]
20. Hájek, M. Environmental Optimization of Road Design. Ph.D. Thesis, University of Zilina, Zilina, Slovakia. *in progress*.
21. Komačka, J.; Remišová, E.; Liu, G.; Leegwater, G.; Nielsen, E. Influence of Reclaimed Asphalt with Polymer Modified Bitumen on Properties of Different Asphalts for a Wearing Course. In *Sustainability, Eco-Efficiency and Conservation in Transportation Infrastructure Asset Management, Proceedings of the 3rd International Conference on Transportation Infrastructure, Pisa, Italy, 22–25 April 2014*; Taylor & Francis Group: London, UK, 2014; pp. 179–185.
22. Lima, M.S.S.; Hajibabaei, M.; Hesarkazzazi, S.; Sitzenfrei, R.; Buttgereit, A.; Queiroz, C.; Tautschnig, A.; Gschösser, F. Environmental Potentials of Asphalt Materials Applied to Urban Roads: Case Study of the City of Münster. *Sustainability* **2020**, *12*, 6113. [CrossRef]
23. Varma, S.; Jamrah, A.; Kutay, M.E.; Korkmaz, K.A.; Haider, S.W.; Buch, N. A Framework Based on Engineering Performance and Sustainability to Assess the Use of New and Recycled Materials in Pavements. *Road Mater. Pavement Des.* **2019**, *20*, 1844–1863. [CrossRef]
24. Bolden, J.; Abu-Lebdeh, T.; Fini, E. Utilization of Recycled and Waste Materials in Various Construction Applications. *Am. J. Environ. Sci.* **2013**, *9*, 14–24. [CrossRef]
25. Maciejewski, K.; Ramiaczek, P.; Remisova, E. Effects of Short-Term Ageing Temperature on Conventional and High-Temperature Properties of Paving-Grade Bitumen with Anti-Stripping and Wma Additives. *Materials* **2021**, *14*, 6229. [CrossRef]
26. D'Angelo, J.; Harm, E.; Bartoszek, J.; Baumgardner, G.; Corrigan, M.; Cowsert, J.; Harman, T.; Jamshidi, M.; Jones, W.; Newcomb, D.; et al. *Warm-Mix Asphalt: European Practice*; U.S. Department of Transportation: Washington, DC, USA, 2008.
27. Falliano, D.; de Domenico, D.; Ricciardi, G.; Gugliandolo, E. Compressive and Flexural Strength of Fiber-Reinforced Foamed Concrete: Effect of Fiber Content, Curing Conditions and Dry Density. *Constr. Build. Mater.* **2019**, *198*, 479–493. [CrossRef]

28. Van Dijk, S. *Foamed Concrete: A Dutch View*; British Cement Association: Camberley, UK, 1991.
29. Amran, Y.H.M.; Farzadnia, N.; Ali, A.A.A. Properties and Applications of Foamed Concrete; a Review. *Constr. Build. Mater.* **2015**, *101*, 990–1005. [[CrossRef](#)]
30. Yang, K.H.; Lee, K.H.; Song, J.K.; Gong, M.H. Properties and Sustainability of Alkali-Activated Slag Foamed Concrete. *J. Clean. Prod.* **2014**, *68*, 226–233. [[CrossRef](#)]
31. Wei, S.; Yiqiang, C.; Yunsheng, Z.; Jones, M.R. Characterization and Simulation of Microstructure and Thermal Properties of Foamed Concrete. *Constr. Build. Mater.* **2013**, *47*, 1278–1291. [[CrossRef](#)]
32. Kim, H.K.; Jeon, J.H.; Lee, H.K. Workability, and Mechanical, Acoustic and Thermal Properties of Lightweight Aggregate Concrete with a High Volume of Entrained Air. *Constr. Build. Mater.* **2012**, *29*, 193–200. [[CrossRef](#)]
33. Fu, Y.; Wang, X.; Wang, L.; Li, Y. Foam Concrete: A State-of-the-Art and State-of-the-Practice Review. *Adv. Mater. Sci. Eng.* **2020**, *2020*, 6153602. [[CrossRef](#)]
34. Falliano, D.; de Domenico, D.; Ricciardi, G.; Gugliandolo, E. Improving the Flexural Capacity of Extrudable Foamed Concrete with Glass-Fiber Bi-Directional Grid Reinforcement: An Experimental Study. *Compos. Struct.* **2019**, *209*, 45–59. [[CrossRef](#)]
35. Vlcek, J.; Drusa, M.; Scherfel, W.; Sedlar, B. Experimental Investigation of Properties of Foam Concrete for Industrial Floors in Testing Field. *IOP Conf. Ser. Earth Environ. Sci.* **2017**, *95*, 022049. [[CrossRef](#)]
36. Kadela, M.; Kozłowski, M.; Kukielka, A. Application of Foamed Concrete in Road Pavement—Weak Soil System. *Procedia Eng.* **2017**, *193*, 439–446. [[CrossRef](#)]
37. Hulimka, J.; Krzywoń, R.; Jędrzejewska, A. Laboratory Tests of Foam Concrete Slabs Reinforced with Composite Grid. *Procedia Eng.* **2017**, *193*, 337–344. [[CrossRef](#)]
38. Izvolt, L.; Dobes, P.; Drusa, M.; Kadela, M.; Holesova, M. Experimental and Numerical Verification of the Railway Track Substructure with Innovative Thermal Insulation Materials. *Materials* **2022**, *15*, 160. [[CrossRef](#)]
39. Act No. 135/1961, Act on Roads (Road Law), Slovak Government, Bratislava, Slovakia, 1961, Coll. on Roads (Road Act). Available online: <https://www.zakonypreludi.sk/zz/1961-135> (accessed on 7 June 2022).
40. Keeling, R.C. *Design of Flexible Pavements Using the Triaxial Compression Test*; Highway Research Board Bulletin: Washington, DC, USA, 1947.
41. Barber, E.S. Application of Triaxial Compression Test Results to the Calculation of Flexible Pavement Thickness. In Proceedings of the Twenty-Sixth Annual Meeting of the Highway Research Board, Washington, DC, USA, 5–8 December 1946; Volume 26, pp. 26–39.
42. McLeod, N.W. *Flexible Pavement Thickness Requirements*; Proceedings; AAPT: Cleveland, OH, USA, 1956; Volume 25.
43. Ullidtz, P. *Pavement Analysis. Developments in Civil Engineering*; Elsevier Science Ltd.: Amsterdam, The Netherlands, 1987; Volume 19, ISBN 0444428178.
44. Duncan, J.M.; Monismith, C.L.; Wilson, E.L. Finite Element Analysis of Pavements. *Highw. Res. Rec.* **1968**, *228*, 157.
45. Cho, Y.H.; McCullough, B.F.; Weissmann, J. Considerations on Finite-Element Method Application in Pavement Structural Analysis. *Transp. Res. Rec.* **1996**, *1539*, 96–101. [[CrossRef](#)]
46. Yin, H.; Stoffels, S.; Solaimanian, M. Optimization of Asphalt Pavement Modeling Based on the Global-Local 3D FEM Approach. *Road Mater. Pavement Des.* **2008**, *9*, 345–355. [[CrossRef](#)]
47. Jiang, X.; Zeng, C.; Gao, X.; Liu, Z.; Qiu, Y. 3D FEM Analysis of Flexible Base Asphalt Pavement Structure under Non-Uniform Tyre Contact Pressure. *Int. J. Pavement Eng.* **2019**, *20*, 999–1011. [[CrossRef](#)]
48. Hájek, M.; Decký, M.; Scherfel, W. Objectification of Modulus Elasticity of Foam Concrete Poroflow 17-5 on the Subbase Layer. *Civ. Environ. Eng.* **2016**, *12*, 55–62. [[CrossRef](#)]
49. Hajek, M.; Decky, M.; Drusa, M.; Oriniová, L.; Scherfel, W. Elasticity Modulus and Flexural Strength Assessment of Foam Concrete Layer of Poroflow. *IOP Conf. Ser. Earth Environ. Sci.* **2016**, *44*, 022021. [[CrossRef](#)]
50. Decky, M.; Scherfel, W.; Remisova, E.; Sramek, J.; Zgutova, K.; Vangel, J.; Plesnik, J. *Sustainable Materials and Technologies for the Pavement Construction and Reinforcement of Traffic Areas*; University of Zilina, EDIS—Publishing Center: Zilina, Slovakia, 2021.
51. Sinnhuber, K.A. Central Europe: Mitteleuropa: Europe Centrale: An Analysis of a Geographical Term. *Trans. Pap. (Inst. Br. Geogr.)* **1954**, *29*, 15–39. [[CrossRef](#)]
52. Pynsent, R.B. Tinkering with the Ferkos: A Kind of Slovakness. *Slavon. East Eur. Rev.* **1998**, *76*, 279–295.
53. Petritsch, W. Culture in Central Europe: Possibilities and Preconditions. *Anal.-Cent. East. Eur. Rev.-Engl. Ed.* **2008**, *1*, 131–140.
54. Wikipedia. Available online: https://En.Wikipedia.Org/Wiki/Central_Europe (accessed on 6 June 2022).
55. STN EN 12390-5:2020; Testing Hardened Concrete. Part 5: Flexural Strength of Test Specimens. Slovak Standard; Slovak Office of Standards, Metrology and Testing: Bratislava, Slovakia, 2020. (In Slovak)
56. Wikipedia. Available online: https://En.Wikipedia.Org/Wiki/Geographical_midpoint_of_Europe (accessed on 6 June 2022).
57. Decky, M.; Papanova, Z.; Juhas, M.; Kudelcikova, M. Evaluation of the Effect of Average Annual Temperatures in Slovakia between 1971 and 2020 on Stresses in Rigid Pavements. *Land* **2022**, *11*, 764. [[CrossRef](#)]
58. Zuzulova, A. *TP 098 Cement Concrete Pavement Design on Road Network*; Technological Standard of Ministry of Transport; Construction and Regional Development of the Slovak Republic, Section for Road Transport and Roads, Slovak Road Administration: Bratislava, Slovakia, 2015.
59. STN 73 6114; Pavement of Roads; Basic Provision for Structural Design. Slovak Standard; Slovak Office of Standards, Metrology and Testing: Bratislava, Slovakia, 1997. (In Slovak)

60. Decký, M.; Drusa, M.; Pepucha, L.; Zgútová, K. *Earth Structures of Transport Constructions*, 1st ed.; Pearson Educ. Ltd.: Harlow, UK, 2013; ISBN 978-1-78399-925-5.
61. De Normalisation, C.E. *EN 12390-5: Testing Hardened Concrete—Part 5: Flexural Strength of Test Specimens*; CEN: Brussels, Belgium, 2009.
62. Ramamurthy, K.; Kunhanandan Nambiar, E.K.; Indu Siva Ranjani, G. A Classification of Studies on Properties of Foam Concrete. *Cem. Concr. Compos.* **2009**, *31*, 388–396. [[CrossRef](#)]
63. Raj, A.; Sathyan, D.; Mini, K.M. Physical and Functional Characteristics of Foam Concrete: A Review. *Constr. Build. Mater.* **2019**, *221*, 787–799. [[CrossRef](#)]
64. Rahman, M.T.; Mahmud, K.; Ahsan, S. Stress-Strain Characteristics of Flexible Pavement Using Finite Element Analysis. *Int. J. Civ. Struct. Eng.* **2011**, *2*, 233–240.
65. Reiterman, P.; Davidová, V.; Machovec, J.; Šulc, R. Freeze-Thaw Resistance of the Pavement with High Replacement of Portland Cement. *AIP Conf. Proc.* **2021**, *2322*, 020027.
66. Webster, K. *The Circular Economy a Wealth of Flows*; Ellen MacArthur Foundation Publishing: Cowes, UK, 2017.
67. Spišáková, M.; Mandičák, T.; Mésároš, P.; Špak, M. Waste Management in a Sustainable Circular Economy as a Part of Design of Construction. *Appl. Sci.* **2022**, *12*, 4553. [[CrossRef](#)]
68. Pohoryles, D.A.; Bournas, D.A. A Unified Macro-Modelling Approach for Masonry-Infilled RC Frames Strengthened with Composite Materials. *Eng. Struct.* **2020**, *223*, 111161. [[CrossRef](#)]
69. Vaitkus, A.; Gražulyte, J.; Skrodenis, E.; Kravcovas, I. Design of Frost Resistant Pavement Structure Based on Road Weather Stations (RWSs) Data. *Sustainability* **2016**, *8*, 1328. [[CrossRef](#)]
70. Nazarko, J.; Radziszewski, P.; Dębkowska, K.; Ejdyś, J.; Gudanowska, A.; Halicka, K.; Kilon, J.; Kononiuk, A.; Kowalski, K.J.; Król, J.B.; et al. Foresight Study of Road Pavement Technologies. *Procedia Eng.* **2015**, *122*, 129–136. [[CrossRef](#)]
71. Schneck, H.; Albrecht, W.; Eisenmann, J.; Jacobs, J.; Kloss, E.W.; Melior, H.; Schneider, W.; Schuster, F.O.; Wehner, B. CONCRETE PAVEMENTS, WEST GERMANY. In Proceedings of the XIVth World Road Congress, Prague, Czechoslovakia; 1971. Available online: <https://trid.trb.org/view/137360> (accessed on 7 June 2022).
72. Weninger-Vycudil, A.; Simanek, P.; Molzer, C.; Litzka, J. Actual Researches on the Austrian PMS-Sector. In Proceedings of the 6th International Conference on Managing Pavements, Brisbane, Australia, 19–24 October 2004.
73. Dhand, V.; Mittal, G.; Rhee, K.Y.; Park, S.J.; Hui, D. A Short Review on Basalt Fiber Reinforced Polymer Composites. *Compos. Part B Eng.* **2015**, *73*, 166–180. [[CrossRef](#)]
74. Jiang, J.; Jiang, C.; Li, B.; Feng, P. Bond Behavior of Basalt Textile Meshes in Ultra-High Ductility Cementitious Composites. *Compos. Part B Eng.* **2019**, *174*, 107022. [[CrossRef](#)]
75. Bieliatynskyi, A.; Krayushkina, K.; Breskich, V.; Lunyakov, M. Basalt Fiber Geomats—Modern Material for Reinforcing the Motor Road Embankment Slopes. *Transp. Res. Procedia* **2021**, *54*, 744–757. [[CrossRef](#)]
76. Sarkar, A.; Hajihosseini, M. The Effect of Basalt Fibre on the Mechanical Performance of Concrete Pavement. *Road Mater. Pavement Des.* **2020**, *21*, 1726–1737. [[CrossRef](#)]
77. Krzywoń, R.; Hulimka, J.; Jędrzejewska, A.; Górski, M. Application of Fibre Composite Grids as Reinforcement of Foamed PC and GP Concrete. *MATEC Web Conf.* **2019**, *274*, 05002. [[CrossRef](#)]
78. Hájek, M.; Decký, M. Homomorphic Model Pavement with Sub Base Layer of Foam Concrete. *Procedia Eng.* **2017**, *192*, 283–288. [[CrossRef](#)]
79. Decký, M.; Drusa, M.; Zgútová, K.; Blaško, M.; Hájek, M.; Scherfel, W. Foam Concrete as New Material in Road Constructions. *Procedia Eng.* **2016**, *161*, 428–433. [[CrossRef](#)]